Exploiting Shadowing Stationarity for Antenna Selection in V2V Communications

Petros S. Bithas, *Member, IEEE*, Athanasios G. Kanatas, *Senior Member, IEEE*, and David W. Matolak, *Senior Member, IEEE*

***Abstract*—Antenna selection (AS) techniques are considered as ideal candidates for vehicle-to-vehicle (V2V) communications, since they improve system's performance and simultaneously satisfy the hardware and signal processing constraints that exist in these systems. However, the achieved gain over single antenna links is affected by the fast varying wireless channel, since AS is frequently performed using outdated versions of the signal-to-noise ratio (SNR). In this paper, we propose an AS technique that exploits the stationarity of large-scale fading. In this context, by employing shadowing information as an AS criterion, the negative consequences of the outdated channel state information (CSI) can be alleviated, since large-scale fading varies more slowly than small-scale fading. The performance of the proposed technique is analyzed using the criteria of outage probability and average output SNR. It is shown that the proposed scheme outperforms the corresponding one that is based on outdated CSI, especially in scenarios with mild fading/shadowing channel conditions. Moreover, the influence of correlated shadowing on the system's performance has been also analytically investigated. The main results have been also verified by empirical data based on measurement campaigns in non-stationary communication conditions.**

***Index Terms*—Composite fading, correlated shadowing, empirical CDF, low complexity V2V communications, shadowing stationarity, transmit/receive antenna selection.**

I. Introduction

VEHICLE-to-vehicle (V2V) communication systems are expected to be one of the pillars towards enabling the autonomous driving in future intelligent transportation systems (ITSs). By integrating these systems in vehicles, several clear benefits will be attained, including enhanced safety and mobility, reduced traffic emissions, as well as improved infotainment. However, the direct application of advanced techniques developed mainly for cellular communication systems, will not result to the promised performance improvements in the case of V2V communication systems. Reasons for this undesirable ascertainment are attributable to the following: the peculiarities of the wireless medium in vehicular communications (fast changes of the environmental conditions and the mobility of both the transmitter (Tx) and the receiver (Rx)), the constraints that exist when integrating these systems on real vehicles, i.e., power and space limitations, and the particular requirements of the V2V applications related to increased reliability and low latency. In that vein, antenna selection (AS) techniques are expected to be an integral part of the V2V communication systems, since they satisfy performance requirements in most of the previous mentioned scenarios, e.g., they increase the overall system's signal-to-noise ratio (SNR) and simultaneously meet the low complexity constraints.

In V2V communications, due to the continuous motion of the Tx, Rx, and the surrounding scatterers, the channel conditions change rapidly. Thus, an AS system whose operation depends on the available channel state information (CSI), in practice operates using outdated versions of CSI. As a result, irreducible diversity gain losses are expected, as it is proved in many studies in the past, e.g., [1], [2]. The performance degradation due to the outdated CSI increases with the speed of vehicle, since higher Doppler shifts arise, which, in limiting scenarios, will result to performance similar to single antenna communication systems.

A quite promising solution to improve this situtation is proposed in [3]. In that paper, a transmit antenna selection (TAS) scheme based on shadowing side information (SSI) was proposed, in which the transmit antenna offering the largest amplitude shadowing variable between the Tx and the Rx is selected. It was shown that as the number of antennas increases, the shadowing effects on the transmitted signal can be eliminated. The same basic idea, regarding AS with SSI, was recently adopted in [4], [5] in physical layer security and cooperative relaying scenarios, respectively. For example, in [5], it was also proved that SSI-based AS is a promising option for communication systems operating in higher frequencies, e.g., in extremely higher frequency bands. Moreover, the utilization of the large-scale fading characteristics has been also examined in [6], where a low-complexity multi-user scheme in massive multiple-input multiple-output (MIMO) scenario is proposed, which offers similar performance with traditional CSI-based schemes. A common outcome in all the above mentioned works, is that the exploitation of the shadowing information, provides worth-studying opportunities towards designing low complexity communication techniques that offer similar performance with existing CSI-based ones. Here, it should be noted that the shadowing effects that are induced by obstructing vehicles between the mobile Tx and Rx considerably affect the performance of intervehicular communication systems [7], [8]. However, very few contributions have analytically investigated the impact of large-scale fading in these systems and the required countermeasures for improving their performance.

Motivated by the aforesaid observations, in this paper, we

P. S. Bithas and A. G. Kanatas are with the Department of Digital Systems, University of Piraeus, 18534 Piraeus, Greece (e-mail: {pbithas, kanatas}@unipi.gr).

D. W. Matolak is with the University of South Carolina, Department of Electrical Engineering, Columbia, SC 29208 USA (email: matolak@sc.edu).

Digital Object Identifier 10.1109/TCOMM.2017.2710196

propose and analytically investigate a TAS/selection diversity (SD) system that exploits the stationarity of the shadowing. The system operates in a composite fading environment, in which small-scale fading and large-scale fading are modeled using the Rice and the Inverse-Gamma (IG) distributions, respectively. The latter one has been recently proposed as an alternative distribution for accuretely modeling the shadowing variable variations [9], [10]. Based on this model, mathematical convenient statistical expressions can be derived, in contrast to the cumbersome expressions that are obtained with lognormal distribution. In this context, important statistical characteristics for this composite model are derived in closed form for a single-input single-output (SISO) communication system. The analysis is then extended to the scenario where multiple antennas exist at both the Tx and the Rx, where the pair offering the largest amplitude shadowing variable is selected for the communication phase[1]. In the derived results, the generic case where independent but non-identically distributed (i.n.d.) fading/shadowing conditions exist is considered. Simplified expressions are also provided for independent and identically distributed (i.i.d.) conditions. Both these scenarios have been studied in order to prepare a reference point. In addition, in a more realistic research scenario, the influence of correlated shadowing variables has been also analytically investigated. Finally, the empirical data that have been also employed verify i) the appropriateness of the IG distribution to model shadowing variations and ii) the applicability of the proposed scheme in real world situations.

The remainder of the paper is organized as follows. In Section II, the system and channel model of the scheme under consideration is presented. In Section III, a statistical framework for the received SNR has been developed, while in Section IV, the derived analytical results have been used for the performance evaluation. In Section V, representative numerical evaluated results and comparisons with measured data are presented and discussed, while in Section VI, the concluding remarks can be found.

II. System and Channel Model

A. System Model

We consider a communication system in which both the Tx and the Rx are equipped with one radio frequency (RF) chain and N_t, N_r antennas, respectively. Such a low complexity system satisfies the space and hardware constraints that exist in vehicular communication systems. The links between the Tx and the Rx are simultaneously affected by small-scale fading (or multipath fading) and shadowing (or large-scale fading). In this context, the composite envelope of the received signal between the Tx antenna i and the Rx antenna j is denoted as $c_{i,j}$ and the received SNR is given by [11]

$$\gamma_{i,j} = c_{i,j}^2 \frac{E_s}{N_0} = h_{i,j}^2 s_{i,j}^2 \frac{E_s}{N_0} = g_{i,j} p_{i,j}, \tag{1}$$

where $h_{i,j}$ and $s_{i,j}$ denote the amplitude of the smale-scale fading and shadowing variables, respectively, $g_{i,j} = h_{i,j}^2, p_{i,j} = s_{i,j}^2 \frac{E_s}{N_0}$, E_s is the average energy per transmitted symbol, and N_0 the power spectral density of the additive white Gaussian noise. In traditional CSI-based AS schemes that operate in V2V communication environments, the estimated channel condition at the selection phase, could be significantly different to the corresponding one at the reception instance, due to the fast variations of the wireless medium. In particular, even at the ideal scenario where the feedback interval T_D is equal or less than channel's coherence time T_c, i.e., the duration within the channel is approximately constant, a delayed version of the CSI will be available, as it is shown in Fig. 1. An alternative approach is to select the antenna by taking advantage of the information related to the shadowing conditions [3]. This approach is mainly based on the fact that the decorrelation distance of the large-scale fading is two orders of magnitude larger than the one of the small-scale fading [12]. This is also shown in Fig. 1, where T_c and stationarity time, i.e., the duration in which signal power remains constant, are depicted. Therefore, with stationarity- (or SSI-) based AS, the antennas pair that is selected is the one providing the maximum averaged received power, i.e., shadowing variable, over a predetermined time interval. After the ℓ, κth antenna-pair is selected, the corresponding index is fed back to the Tx in order to proceed with the signal transmission. Thus, the received SNR can be expressed as

$$\gamma_{\ell,\kappa} = g_{\ell,\kappa} \max_{\substack{1\le i\le N_t \\ 1\le j\le N_r}} \{p_{i,j}\} = g_{\ell,\kappa} p_{\max}, \tag{2}$$

where $g_{\ell,\kappa}$ depends on the small-scale fading of the selected pair. It is worth-noting that $g_{\ell,\kappa}$s change in every channel's coherence time, whereas $p_{i,j}$s do not.

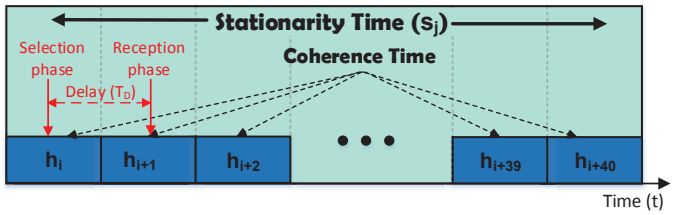

Fig. 1. Stationarity and coherence times in a V2V communication scenario.

B. Channel Model

1) Marginal Statistics: In this paper, small-scale fading is modeled by the Rice distribution, while shadowing is modeled by the IG distribution. This channel model corresponds to scenarios, in which line-of-sight (LoS) conditions co-exist with shadowing by large objects such as buildings and/or other vehicles [13]. Then, the probability density function (PDF) of $g_{i,j}$ is given by [14, eq. (2.16)]

$$f_{g_{i,j}}(x) = \frac{(k_{i,j}+1)}{\Omega} \exp\left(-k_{i,j} - \frac{(k_{i,j}+1)x}{\Omega}\right) \times I_0\left(2\sqrt{\frac{k_{i,j}(k_{i,j}+1)x}{\Omega}}\right), \tag{3}$$

where $k_{i,j}$ corresponds to the ratio of the power of the specular component to the average power of the scattered component,

[1]It is noted that since the shadowing variables vary much slower as compared to the received SNR, it is reasonable to assume that their values at the selection and the reception phases is fully (temporally) correlated.

$\Omega = \mathbb{E}\langle g_{i,j}\rangle$, with $\mathbb{E}\langle\cdot\rangle$ denoting expectation, and $I_v(\cdot)$ denotes the modified Bessel function of the first kind and order v [15, eq. (8.406/1)]. In addition, similar to [9], the shadowing variables are assumed to follow the IG distribution, with PDF given by

$$f_{p_{i,j}}(y) = \frac{\overline{\gamma}_{i,j}^{\alpha_{i,j}}}{\Gamma(\alpha_{i,j}) y^{\alpha_{i,j}+1}} \exp\left(-\frac{\overline{\gamma}_{i,j}}{y}\right), \tag{4}$$

where $\alpha_{i,j} > 1$ is the shaping parameter of the distribution related to the severity of the shadowing, $\overline{\gamma}_{i,j}$ denotes the scaling parameter depicting the average received SNR, which is related to the path losses [16], and $\Gamma(\cdot)$ is the gamma function [15, eq. (8.310/1)]. Using the total probability theorem, the PDF of the instantaneous received SNR of the i,jth pair is given by

$$f_{\gamma_{i,j}}(\gamma) = \int_0^\infty f_{g_{i,j}}(\gamma|y) f_{p_{i,j}}(y) dy. \tag{5}$$

Substituting (3) and (4) in (5) and using [15, eq. (6.643/2)], the following expression is derived

$$\begin{aligned} f_{\gamma_{i,j}}(\gamma) &= \frac{(k_{i,j}+1)^{1/2} \exp(-k_{i,j}) \overline{\gamma}_{i,j}^{\alpha_{i,j}} \alpha_{i,j}}{\sqrt{k_{i,j}\gamma}\left[(k_{i,j}+1)\gamma + \overline{\gamma}_{i,j}\right]^{\alpha_{i,j}+1/2}} \\ &\times \exp\left[\frac{k_{i,j}(k_{i,j}+1)\gamma}{2((k_{i,j}+1)\gamma + \overline{\gamma}_{i,j})}\right] \\ &\times M_{-\alpha_{i,j}-\frac{1}{2},0}\left[\frac{k_{i,j}(k_{i,j}+1)\gamma}{(k_{i,j}+1)\gamma + \overline{\gamma}_{i,j}}\right], \end{aligned} \tag{6}$$

where $M_{\kappa,\mu}(\cdot)$ denotes the Whittaker function [15, eq. (9.220/2)]. The corresponding cumulative distribution function (CDF) expression is given by

$$\begin{aligned} F_{\gamma_{i,j}}(\gamma) &= \frac{(k_{i,j}+1)\gamma}{(k_{i,j}+1)\gamma + \overline{\gamma}_{i,j}} \exp\left[-\frac{k_{i,j}\overline{\gamma}_{i,j}}{(k_{i,j}+1)\gamma + \overline{\gamma}_{i,j}}\right] \\ &\times \sum_{k_1=0}^{\alpha_{i,j}-1} \left[\frac{\overline{\gamma}_{i,j}}{(k_{i,j}+1)\gamma + \overline{\gamma}_{i,j}}\right]^{k_1} L_{k_1}\left[-\frac{k_{i,j}(k_{i,j}+1)\gamma}{(k_{i,j}+1)\gamma + \overline{\gamma}_{i,j}}\right], \end{aligned} \tag{7}$$

where $L_n(\cdot)$ denotes the Laguerre polynomial [15, eq. (8.970)].

2) Bivariate Statistics: Assuming that $p_{i,j}, \tilde{p}_{i,j}$ denote two IG distributed random variables (RVs) with marginal PDF given by (4). By making a change of variables in [14, eq. (6.1)], the joint PDF of $p_{i,j}, \tilde{p}_{i,j}$ can be expressed as

$$\begin{aligned} f_{p_{i,j},\tilde{p}_{i,j}}(x,y) &= \frac{\left(\overline{\gamma}_{i,j}\overline{\overline{\gamma}}_{i,j}\right)^{\frac{\alpha_{i,j}+1}{2}}}{\Gamma(\alpha_{i,j})(1-\rho)\rho^{\frac{\alpha_{i,j}-1}{2}}(xy)^{m+3}} \\ &\times \exp\left[-\frac{\overline{\overline{\gamma}}_{i,j}/x + \overline{\gamma}_{i,j}/y}{(1-\rho)}\right] I_{\alpha_{i,j}-1}\left[\frac{2\sqrt{\rho\overline{\gamma}_{i,j}\overline{\overline{\gamma}}_{i,j}}}{(1-\rho)(xy)^{\frac{1}{2}}}\right], \end{aligned} \tag{8}$$

where ρ denotes the correlation coefficient between $p_{i,j}, \tilde{p}_{i,j}$ and $\overline{\overline{\gamma}}_{i,j}$ denotes the scaling parameter of $\tilde{p}_{i,j}$. The corresponding joint CDF expression can be obtained by employing the infinite series representation of the Bessel function [15, eq. (8.445)] and performing a mathematical analysis resulting to

$$\begin{aligned} F_{p_{i,j},\tilde{p}_{i,j}}(x,y) &= (1-\rho)^{\alpha_{i,j}} \sum_{t=0}^{\infty} \frac{\rho^t}{\Gamma(\alpha_{i,j})\Gamma(\alpha_{i,j}+t)t!} \\ &\times \Gamma\left(\alpha_{i,j}+t, \frac{\left(\overline{\gamma}\overline{\overline{\gamma}}\right)^{\frac{1}{2}}}{(1-\rho)x^{\frac{1}{2}}}\right) \Gamma\left(\alpha_{i,j}+t, \frac{\left(\overline{\gamma}\overline{\overline{\gamma}}\right)^{\frac{1}{2}}}{(1-\rho)y^{\frac{1}{2}}}\right), \end{aligned} \tag{9}$$

with $\Gamma(\cdot,\cdot)$ denoting the upper incomplete gamma function [15, eq. (8.350/2)]. The CDF in (9) converges fast, since in most cases a relatively small number of terms is sufficient, i.e., < 20, to achieve a high accuracy. To the best of the authors' knowledge, both (8) and (9) have never been reported in the open technical literature.

III. TAS/SD Statistics

A. Independent and Non-Identically Distributed Conditions

Here, the idealized case where i.n.d. fading/shadowing conditions exist is investigated. This scenario can be used as a bound to more realistic ones, in which identical and/or correlated conditions exist. In this context, the CDF expression of the instantaneous received SNR of the selected pair $\gamma_{\ell,\kappa}$ is given by

$$F_{\gamma_{\ell,\kappa}}(\gamma) = 1 - \sum_{i,j=1}^{N_t,N_r} \sum_{\substack{q_{x,y}=1 \\ x,y\neq i,j}}^{\alpha_{x,y}-1} \frac{\mathcal{S}_{i,j}}{\Gamma(\alpha_{i,j})\overline{\gamma}_{i,j}^{-\alpha_{i,j}}} \mathcal{I}(\gamma). \tag{10}$$

The proof for (10), as well as the definition of $\mathcal{I}(\gamma), \mathcal{S}_{i,j}$, and the sums are given in Appendix A. The corresponding PDF is given by

$$\begin{aligned} f_{\gamma_{\ell,\kappa}}(\gamma) &= \sum_{i,j=1}^{N_tN_r} \sum_{\substack{q_{x,y}=1 \\ x,y\neq i,j}}^{\alpha_{x,y}-1} \frac{\exp(-k_{\ell,\kappa})}{\Gamma(\alpha_{i,j})\overline{\gamma}_{i,j}^{-\alpha_{i,j}}} \frac{\mathcal{S}_{i,j}(k_{\ell,\kappa}+1)}{\left[(k_{\ell,\kappa}+1)\gamma + B\right]^h} \\ &\times \Gamma(a)\pi \exp\left(\frac{k_{\ell,\kappa}(k_{\ell,\kappa}+1)\gamma}{B + (k_{\ell,\kappa}+1)\gamma}\right) \sum_{t=0}^{h-1} \frac{(1-h)_t}{t!(1)_t} \\ &\times \left(-\frac{k_{\ell,\kappa}(k_{\ell,\kappa}+1)\gamma}{(k_{\ell,\kappa}+1)\gamma + B}\right)^t, \end{aligned} \tag{11}$$

where h, B are defined in Appendix A and $(z)_n$ denotes the Pochhammeer symbol [17, eq. (6.1.22)]. The total CDF of the output SNR is given by

$$F_{\gamma_{\text{out}}}(\gamma) = \sum_{\ell=1}^{N_t} \sum_{\kappa=1}^{N_r} P_{\ell,\kappa} F_{\gamma_{\ell,\kappa}}(\gamma), \tag{12}$$

in which $P_{\ell,\kappa}$ can be evaluated as

$$P_{\ell,\kappa} = \sum_{\substack{q_{x,y}=1 \\ x,y\neq i,j}}^{\alpha_{x,y}-1} \frac{S_{\ell,\kappa}\overline{\gamma}^{\alpha_{\ell,\kappa}}}{\Gamma(\alpha_{\ell,\kappa})} \frac{\Gamma(h-1)}{B^{h-1}}. \tag{13}$$

The proof is given in Appendix B.

B. Independent and Identically Distributed Conditions

For i.i.d. fading/shadowing, i.e., assuming that $\alpha_{i,j} = \alpha, \overline{\gamma}_{i,j} = \overline{\gamma}, k_{i,j} = k$, the CDF expression of γ_{out} is given by

$$F_{\gamma_{\text{out}}}(\gamma) = 1 - \sum_{\substack{n_1,n_2,\ldots,n_\alpha=1 \\ n_1+\cdots+n_\alpha=N_{t,r}-1}}^{N_{t,r}-1} \frac{(b-2)!}{\Gamma(\alpha)N_{t,r}^{b-2}} \times \left\{1 - \frac{\gamma(k+1)}{N_{t,r}\overline{\gamma}+(k+1)\gamma}\exp\left[-\frac{kN_{t,r}\overline{\gamma}}{N_{t,r}\overline{\gamma}+\gamma(k+1)}\right] \times \sum_{t=0}^{b-2}\left[\frac{N_{t,r}\overline{\gamma}}{N_{t,r}\overline{\gamma}+\gamma(k+1)}\right]^t L_t\left[-\frac{k(k+1)\gamma}{N_{t,r}\overline{\gamma}+\gamma(k+1)}\right]\right\}, \tag{14}$$

where

$$\sum_{\substack{n_1,n_2,\ldots,n_\alpha=1 \\ n_1+\cdots+n_\alpha=N_{t,r}-1}}^{N_{t,r}-1} = \sum_{\substack{n_1=0}}^{N_{t,r}-1}\sum_{\substack{n_2=0 \\ n_1+n_2+\cdots+n_\alpha=N_{t,r}-1}}^{N_{t,r}-1}\cdots\sum_{n_\alpha=0}^{N_{t,r}-1}\frac{\Gamma(N_{t,r})/\left(n_1!\cdots n_\alpha!\right)}{(0!)^{n_1}\cdots((\alpha-1)!)^{n_\alpha}},$$

$N_{t,r} = N_tN_r$, and $b = \sum_{j=2}^{\alpha}(j-1)n_j + \alpha + 1$. For deriving (14), a convenient expression for the PDF of $p_{\max}$ is required, which, in general, is defined as $f_{p_{\max}}(y) = N_{t,r}f_{p_{i,j}}(y)F_{p_{i,j}}(y)^{N_{t,r}-1}$. Substituting (4) and (A-4) in this definition and employing the multinomial identity, the following simplified expression is extracted

$$f_{p_{\max}}(y) = \frac{N_{t,r}}{\Gamma(\alpha)}\exp\left(-\frac{N_{t,r}\overline{\gamma}}{y}\right)\sum_{\substack{n_1,n_2,\ldots,n_\alpha=1 \\ n_1+\cdots+n_\alpha=N_{t,r}-1}}^{N_{t,r}-1}\frac{\overline{\gamma}^{b-1}}{y^b}. \tag{15}$$

Based on (15) and using a similar approach as the one presented in Appendix A, finally yields (14). The corresponding expression for the PDF of γ_{out} is given by

$$f_{\gamma_{\text{out}}}(\gamma) = \frac{N_{t,r}}{\Gamma(\alpha)}\sum_{\substack{n_1,n_2,\ldots,n_\alpha=1 \\ n_1+\cdots+n_\alpha=N_{t,r}-1}}^{N_{t,r}-1}\exp\left[\frac{k(k+1)\gamma}{N_{t,r}\overline{\gamma}+(k+1)\gamma}\right] \times \frac{(k+1)\Gamma(b)\overline{\gamma}^{b-1}e^{-k}}{\left(N_{t,r}\overline{\gamma}+(k+1)\gamma\right)^b}\sum_{p=0}^{b-1}\frac{(1-b)_p}{p!(1)_p}\left[\frac{-k(k+1)\gamma}{N_{t,r}\overline{\gamma}+(k+1)\gamma}\right]^p. \tag{16}$$

C. Spatial Correlation Conditions

In real communication environments, shadowing spatial correlation will be present, affecting the performance of the systems [18]. Thus, the previous analysis will be extended to the scenario where correlation in shadowing exists. In particular, we consider a communication system with $N_t = 2$ and $N_r = 1$[2], in which the received shadowing variables are correlated with joint PDF given by (8). For identically distributed small- and large-scale fading, i.e., $\alpha_{i,j} = \alpha, \overline{\gamma}_{i,j} = \overline{\overline{\gamma}}_{i,j} = \overline{\gamma}, k_{i,j} = k$, the CDF of γ_{out} is given by

$$F_{\gamma_{\text{out}}}(\gamma) = 1 - \sum_{t=0}^{\infty}\sum_{d_1=0}^{\alpha+t-1}\sum_{d_2=0}^{\alpha+t-1}\frac{\rho^t((\alpha+t-1)!)^2(1-\rho)^m}{\Gamma(\alpha)\Gamma(\alpha+t)t!d_1!d_2!} \times \frac{(d_1+d_2)!}{2^{d_1+d_2}}\mathcal{G}(d_1+d_2)\mathcal{G}(d_1+d_2-1) \tag{17}$$

where

$$\mathcal{G}(x) = 1 - \frac{(1+k)\gamma}{(1+k)\gamma+2\overline{\gamma}/(1-\rho)} \times \exp\left[-k\frac{\overline{\gamma}/(1-\rho)}{(1+k)\gamma/2+\overline{\gamma}/(1-\rho)}\right] \times \sum_{q=0}^{x}\left[\frac{\overline{\gamma}/(1-\rho)}{(1+k)\gamma/2+\overline{\gamma}/(1-\rho)}\right]^q \times L_q\left[-k\frac{(1+k)\gamma}{(1+k)\gamma+2\overline{\gamma}/(1-\rho)}\right],$$

with $\mathcal{G}(x) = 0$ if $x < 0$. For deriving (17), an analytical expression for PDF of $p_{\max}$, defined as $f_{p_{\max}}(x) = \frac{dF_{p,\tilde{p}}(x,x)}{dx}$, is required. Substituting (9) in this definition and using [15, eq. (8.352/2)], $f_{p_{\max}}(x)$ is deduced as

$$f_{p_{\max}}(x) = \sum_{t=0}^{\infty}\sum_{d_1=0}^{\alpha+t-1}\sum_{d_2=0}^{\alpha+t-1}\frac{\rho^t[(\alpha+t-1)!]^2(1-\rho)^m}{\Gamma(\alpha)\Gamma(\alpha+t)t!d_1!d_2!} \times \left(\frac{\overline{\gamma}}{1-\rho}\right)^{d_1+d_2}\left[\frac{2\exp\left(-\frac{2\overline{\gamma}}{x(1-\rho)}\right)\overline{\gamma}}{(1-\rho)x^{d_1+d_2+2}} - (d_1+d_2)\frac{\exp\left(-\frac{2\overline{\gamma}}{x(1-\rho)}\right)}{x^{d_1+d_2+1}}\right]. \tag{18}$$

Based on (18) and by using a similar approach as the one presented in Appendix A, finally yields (17).

IV. Performance Analysis

In this section, using the previously derived results, analytical expressions for the outage probability (OP) and the average output SNR (ASNR) are derived.

A. Outage Probability (OP)

OP is defined as the probability that the output SNR falls below a predetermined threshold γ_{T} and it can be evaluated as $P_{\text{out}} = F_{\gamma_{\text{out}}}(\gamma_{\text{T}})$, in which $F_{\gamma_{\text{out}}}(\gamma_{\text{T}})$ is given by (12), for the i.n.d. scenario, (14), for the i.i.d. scenario, and (17), for the correlated scenario.

B. Average Output SNR (ASNR)

The ASNR is a performance measure quantifying system's reliability that can be evaluated as $m_{\gamma_{\text{out}}} = \int_0^{\infty}\gamma f_{\gamma_{\text{out}}}(\gamma)d\gamma$. For i.n.d. fading/shadowing, substituting (11) in this definition,

[2]The same result will also apply for $N_t = 1$ and $N_r = 2$.

employing [15, eq. (8.350/1)] and after some mathematical procedure yields

$$m_{\gamma_{\text{out}}} = \sum_{\ell=1}^{N_t}\sum_{\kappa=1}^{N_r} P_{\ell,\kappa} \sum_{i,j=1}^{N_t N_r} \sum_{\substack{q_{x,y}=1 \\ x,y\neq i,j}}^{\alpha_{x,y}-1} \frac{\mathcal{S}_{i,j}\Gamma(h)\overline{\gamma}^{\alpha_{i,j}}}{\Gamma(\alpha_{i,j})} \sum_{t=0}^{h-1} \times \frac{(1-h)_t}{t!(1)_t} \sum_{d=0}^{t+1} \binom{t+1}{d} \frac{(-1)^{2t+1-d}\gamma(t+h-d-1, k_{\kappa,\ell})}{k_{\kappa,\ell}^{h-d-1} B^{h-1}(k_{\kappa,\ell}+1)}, \tag{19}$$

where $\gamma(\cdot,\cdot)$ is the lower incomplete gamma function [15, eq. (8.350/1)]. For the i.i.d. conditions, (19) simplifies to

$$m_{\gamma_{\text{out}}} = \sum_{\substack{n_1,n_2,\ldots,n_\alpha=1 \\ n_1+\cdots+n_\alpha=N_{t,r}-1}}^{N_{t,r}-1} \frac{\Gamma(b)\overline{\gamma}}{\Gamma(\alpha)} \sum_{p=0}^{b-1} \frac{(1-b)_p}{p!(1)_p(k+1)} \times \sum_{d=0}^{p+1} \binom{p+1}{d} \frac{(-1)^{2p+1-d}\gamma(b+p-d-1,\alpha)}{N_{t,r}^{b-2} k^{b-d-1}}. \tag{20}$$

V. Numerical Results

In this section, several numerically evaluated performance results are provided. First of all, the appropriateness of the IG distribution to model shadowing effects in various communication scenarios was studied. First of all, the vehicle-to-infrastructure (V2I) propgation conditions were investigated. To this aim, the empirical data obtained in the channel measurement campaign presented in [19] are employed. These data were collected in an urban pedestrian propagation environment, with a stationary Tx and a mobile Rx, resulting to time-variant channel characteristics. Based on them, in Fig. 2, the empirical PDF of the signal envelope mean (shadow fading) is plotted as a function of the normalized shadowing amplitude. In the same figure, for comparison purposes, the corresponding PDFs of Gamma, IG, and lognormal distributions are also plotted, using the method of moments to estimate their parameters. It is clearly shown that all PDFs provide excellent fit to the empirical one. Moreover, in our analysis the Kullback-Leibler divergence (KLD) criterion has been adopted [20]. Employing this criterion, the distribution that provides the best fit to the measured data, is the one with the minimum value for the distance d_{KL}. Our analysis showed that $d_{KL} = 1.8, 1.54, 1.7\%$, for Gamma, IG, and lognormal distributions, respectively. Therefore, it is proved that the IG distribution is an excellent model for shadow fading in V2I time-varying scenarios. Secondly, an additional example comparing the IG density to measurement data in V2V shadowing conditions in a highway setting, from [8], was investigated in Fig. 3. In this figure, fits are also shown using the lognormal and gamma densities. For this case, since the data set is somewhat sparse (exhibiting a number of zero histogram counts for several values of shadowing variable), the KLD values are generally large (for all densities), thus we report instead the Kolmogorov-Smirnov (KS) test statistic. These values are KS(IG)=0.028, KS(lognormal)=0.016, and KS(gamma)=0.053. Here the lognormal is slightly better than the IG, but the IG fit is good, and fits better to both the measurement data's distribution mode and the measurement

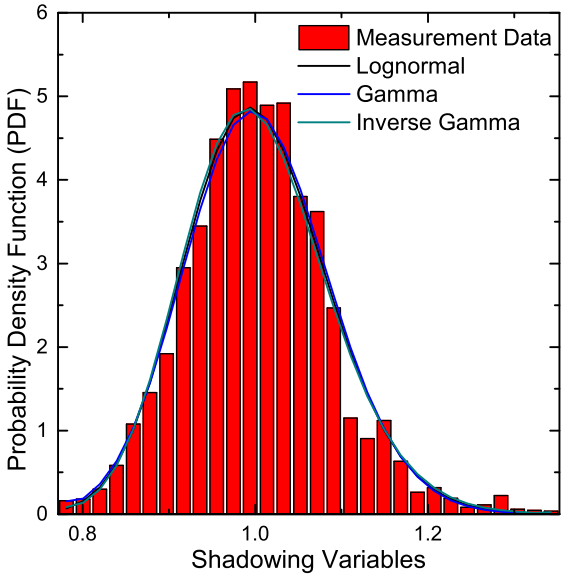

Fig. 2. Empirical and theoretical PDFs comparisons.

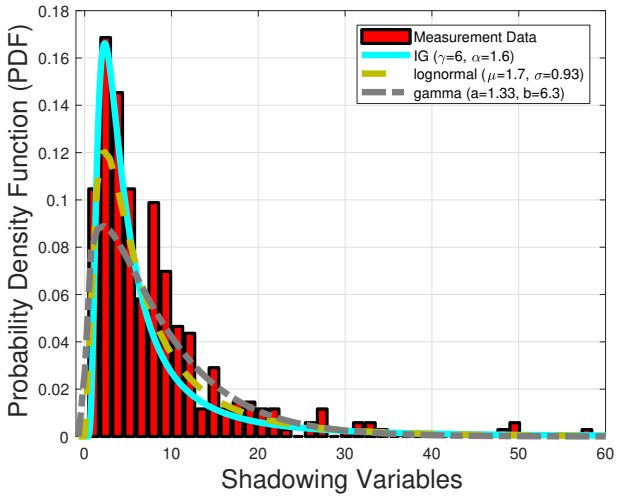

Fig. 3. Empirical and theoretical PDFs comparisons.

distribution tails at the largest values of shadowing variable. Fit rankings using the chi-squared test are comparable. Therefore, from both sets of measurement results it can be concluded that the IG distribution can efficiently model the shadowing in both V2I and V2V communication conditions.

In Fig. 4, assuming $k = 5, \alpha = 2, \overline{\gamma} = 0$dB, the normalized OP is plotted as a function of the outage threshold, γ_T, and for different numbers of the Tx and Rx antennas. It is shown that as the number of the antennas increases, the performance improves with a decreased rate. Moreover, the corresponding performance of the scheme proposed in [3] is also depicted. It is shown that the scheme proposed in this paper outperforms the one presented in [3] as well as the shadowed SISO case, with the later one preserving always the worst performance. It is noteworthy that the proposed scheme can be considered as an effective shadowing countermeasure technique, since it provides better performance, for scenarios with $N_t, N_r \geq 2$, in comparison to a SISO system that operates in a non-shadowing environment. In the same figure, the average output

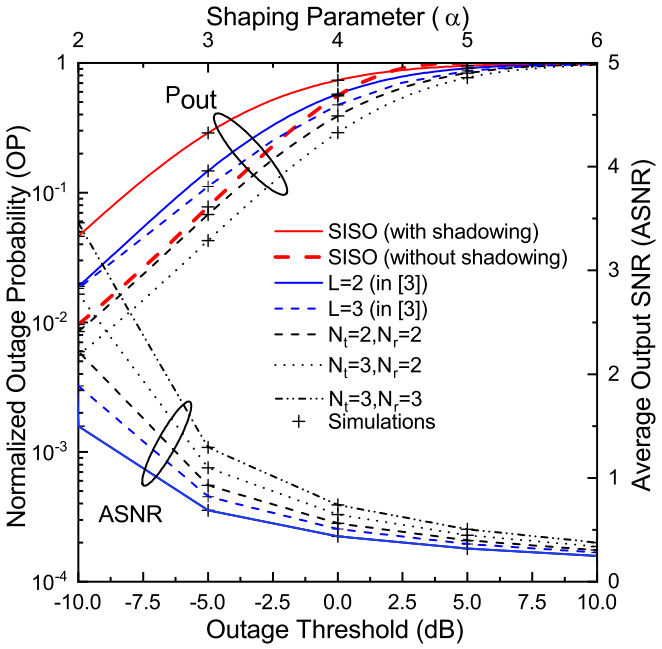

Fig. 4. Normalized outage probability and average output SNR as a function of the outage threshold and α, respectively.

TABLE I
FADING/SHADOWING CONDITIONS FOR FIG. 6.

	Fading	Shadowing
Case 1	k=2 (strong)	α=2 (mild)
Case 2	k=2 (strong)	α=4 (strong)
Case 3	k=8 (mild)	α=2 (mild)
Case 4	k=8 (mild)	α=4 (strong)

SNR is also examined as a function of the shaping parameter α and for different number of Tx/Rx antennas. It is shown that the performance decreases with an increase on α. In Fig. 5, the impact of spatially correlated shadowing on the OP performance has been investigated. In particular, assuming $k = 2, \alpha = 2, N_t = 2, N_r = 1, \overline{\gamma} = 0$dB, the normalized OP is plotted as a function of γ_T and for different values of the shadowing spatial correlation coefficient ρ. It is shown that the performance decreases with the increase of ρ. However, even for relatively high values of ρ, e.g., $\rho \approx 0.7$, the performance improvement of the system under consideration is notable as compared to a SISO system.

Another important investigation that is also performed concerns the performance comparison between SSI- and CSI-based AS schemes, with the latter one being subjected to outdated versions of CSI. In order to perform this comparison, the CDF of the output SNR of a CSI-based TAS scheme operating over Rice/IG composite fading environment is required to be evaluated. However, since an exact analytical expression for this CDF does not exist in the open technical literature, in Appendix C, this CDF has been derived. In Fig. 6, the OP of the proposed scheme and the one that is based on (C-3) is plotted as a function of the temporal

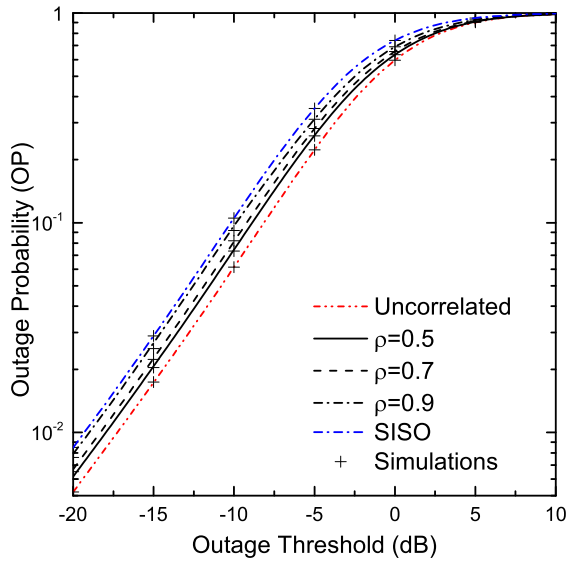

Fig. 5. Outage probability as a function of the outage threshold (γ_T) for different values of the (spatial) correlation coefficient.

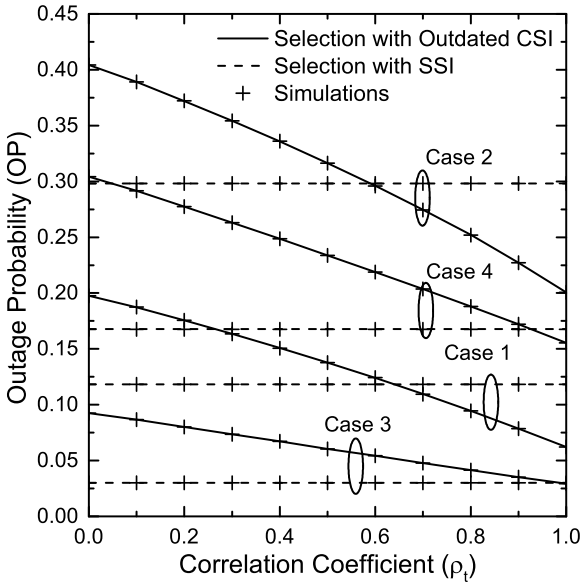

Fig. 6. Outage probability as a function of the correlation coefficient for SSI-, CSI-based antenna selection schemes.

correlation coefficient ρ_t, which quantifies the correlation between the exact and the outdated versions of the received SNR. To obtain this figure, the following assumption was made $N_t = 2, N_r = 1$, while four different scenarios regarding the LoS and fading/shadowing conditions (mild or strong), have been considered and presented in Table I. It is shown that the performance of the CSI-based system improves as ρ_t and k increase as well as with the decrease of α. As a general observation, assuming reasonable values for the time correlation, i.e., $\rho_t > 0.6$, which correspond to regular relative velocities, the CSI-based TAS scheme offers better performance in the cases where strong fading effects are present. This could be explained by the fact that in these scenarios the multipath components are dominant compared to the constant term of the Rice model and thus the technique that offers improved

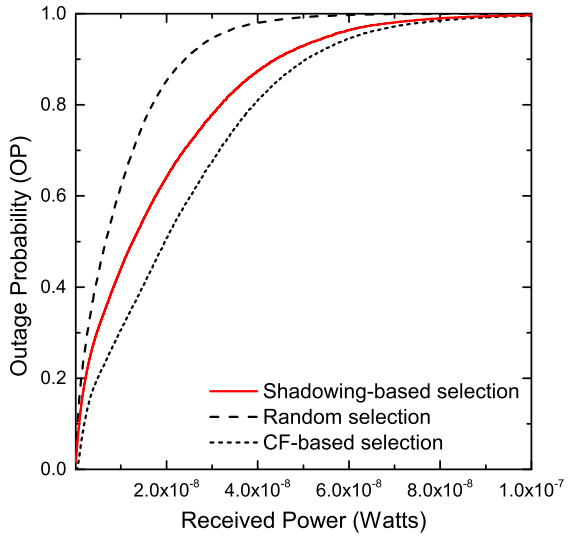

Fig. 7. Empirical outage probability for shadowing-, CF-based, and random channel selection schemes.

fading countermeasure performance is the one that focuses on the selection of the best fading variable, i.e., the CSI-based TAS. However, the proposed scheme outperforms the CSI-based one in all other investigated scenarios, where mild fading conditions and/or lower values of ρ_t exist, which correspond to higher velocities. More specifically, for mild fading/shadowing conditions, i.e., Cases 3 and 4, the proposed scheme provides better performance for almost the entire region of ρ_t. These results reveal that the negative impact of outdated CSI on the system's performance can be alleviated by exploiting the shadowing information. It is noted that the Monte Carlo simulation that have been included in Figs. 4, 5, and 6 verify the validity of the presented theoretical framework.

Finally, in Fig. 7, based on the empirical data for a 2×2 MIMO channel collected in [19], empirical OP comparisons have been performed. In particular, three scenarios have been investigated regarding the adopted channel selection mechanism, namely, i) transmit/receive channel selection based on the composite fading (CF) variables, ii) transmit/receive channel selection based on the shadowing variables, and iii) random channel selection. It should be noted that shadowing-based selection is performed every 10λ, i.e., per stationarity region, in contrast to CF that is performed every $\lambda/20$, i.e., per coherence time. In this figure, it is also depicted the performance improvement induced by the adoption of the shadowing variable selection mechanism as compared to the random channel selection. It is worthwhile to mention that the correlation among the shadowing variables of the empirical data was evaluate to take values between $0.8-0.92$. Therefore, the proposed scheme provides clear benefits even in scenarios where strong correlation effects in shadowing are present.

VI. Conclusions

The performance of a TAS/SD scheme operating in a V2V communication environment in the presence of composite fading has been analytically investigated. The novelty of the proposed scheme lies on the fact that the antenna selection in both sides is performed by exploiting the stationarity of the large-scale fading. Capitalizing on the slow variations of the shadowing variable, the detrimental consequences of the outdated CSI, that is frequently observed in V2V communications, are counteracted. The results presented are based on the derived theoretical analysis, simulations, as well as empirical data. It is shown the appropriateness of the inverse gamma distribution to model the large-scale fading as well as the impact of shadowing correlation on the system's performance. Moreover, it is also proved that in practical situations the proposed approach outperforms the one that uses outdated versions of the CSI, under various fading/shadowing conditions.

Appendix A
Proof for Equation (10)

In this Appendix, the proof for the derivation of (10) is provided. The CDF of $\gamma_{\ell,\kappa}$ can be evaluated by

$$F_{\gamma_{\ell,\kappa}}(\gamma) = \int_0^\infty F_{g_{\ell,\kappa}}(\gamma|y) f_{p_{\max}}(y) dy. \tag{A-1}$$

In (A-1), $F_{g_{\ell,\kappa}}(\gamma|y)$ is given by

$$F_{g_{\ell},\kappa}(\gamma|y) = 1 - Q_1\left(\sqrt{2k_{\ell,\kappa}}, \sqrt{2(k_{\ell,\kappa}+1)\gamma y^{-1}}\right), \tag{A-2}$$

where $Q_1(x,y)$ is the first-order Marcum Q-function [14, eq. (4.33)]. Moreover, based on the order statistics [21], the PDF of $f_{p_{\max}}(y)$ can be derived as

$$f_{p_{\max}}(y) = \sum_{i,j=1}^{N_t N_r} f_{p_{i,j}}(y) \underbrace{\prod_{z_i,z_j=1}^{NtNr} F_{p_{z_1,z_2}}(y)}_{Q_{i,j}}, \tag{A-3}$$

where $\sum_{i,j=1}^{N_t N_r} = \sum_{i=1}^{N_t}\sum_{j=1}^{N_r}$, $\prod_{z_i,z_j=1}^{NtNr} = \prod_{\substack{z_1=1 \\ z_1\neq i \text{ OR} z_2\neq j}}^{N_t}\prod_{z_2=1}^{N_r}$ and

$$F_{p_{z_1,z_2}}(y) = \frac{\Gamma\left(\alpha_{z_1,z_2}, \overline{\gamma}_{z_1,z_2}/y\right)}{\Gamma\left(\alpha_{z_1,z_2}\right)}. \tag{A-4}$$

Based on [15, eq. (8.352/2)], and after a mathematical procedure, the following convenient expression for $Q_{i,j}$ is derived

$$\begin{aligned} Q_{i,j} &= \exp\left(-\sum_{z_i,z_j=1}^{N_t N_r} \frac{\overline{\gamma}_{z_1,z_2}}{y}\right) \prod_{z_i,z_j=1}^{NtNr} \left(\sum_{j=0}^{\alpha_{z_1,z_2}-1} \frac{\left(\frac{\overline{\gamma}_{z_1,z_2}}{y}\right)^j}{j!}\right) \\ &= \sum_{\substack{q_{x,y}=1 \\ x,y\neq i,j}}^{m_{x,y}-1} \mathcal{S}_{i,j} y^{-\sum_{z_i,z_j=1}^{N_t Nr} q_{z_1,z_2}} \exp\left(-\frac{1}{y}\sum_{z_i,z_j=1}^{N_t,N_r} \overline{\gamma}_{z_1,z_2}\right), \end{aligned} \tag{A-5}$$

where

$$\sum_{\substack{q_{x,y}=1 \\ x,y\neq i,j}}^{\alpha_{x,y}-1} = \underbrace{\sum_{q_{1,1}=1}^{\alpha_{1,1}-1} \cdots \sum_{q_{1,N_r}=1}^{\alpha_{1,N_r}-1} \sum_{q_{2,1}=1}^{\alpha_{2,1}-1} \cdots \sum_{q_{x,y}=1}^{\alpha_{x,y}-1} \cdots \sum_{q_{N_t,N_r}=1}^{\alpha_{N_t,N_r}-1}}_{x\neq i \text{ OR } y\neq j},$$

$$\mathcal{S}_{i,j}=\frac{\prod\limits_{z_i,z_j=1}^{N_tN_r}\overline{\gamma}_{z_1,z_2}^{q_{z_1,z_2}}}{q_{1,1}!,\cdots,q_{1,N_r}!q_{2,1}!,\cdots,q_{N_t,N_r}!},\sum_{z_i,z_j=1}^{N_tN_r}=\sum_{\substack{z_1=1\\ z_1\neq i \text{ OR} z_2\neq j}}^{N_t}\sum_{z_2=1}^{N_r}.$$

Substituting (A-5) in (A-3), and (A-3), (4) in (A-1), an integral of the following form appears

$$\mathcal{I}(\gamma)=\int_0^\infty\frac{\exp\left(-B/y\right)}{y^q}Q_1\left[\sqrt{2k_{\ell,\kappa}},\left(\frac{2(k_{\ell,\kappa}+1)\gamma}{y}\right)^{\frac{1}{2}}\right]dy, \tag{A-6}$$

with $q=\alpha_{i,j}+\sum\limits_{z_i,z_j=1}^{N_tN_r}q_{z_1,z_2}+1, B=\sum\limits_{i,j=1}^{N_tN_r}\overline{\gamma}_{i,j}$. This integral can be solved by making a change of variables of the form $z=y^{-1/2}$ and using [22, eq. (8)] yielding to

$$\begin{aligned}\mathcal{I}(\gamma)=2^{q-1}\frac{(q-2)!}{(2B)^{q-1}}&\left[1-\frac{\gamma(k_{\ell,\kappa}+1)}{B+(k_{\ell,\kappa}+1)\gamma}\right.\\&\times\exp\left(-\frac{k_{\ell,\kappa}B}{B+\gamma(k_{\ell,\kappa}+1)}\right)\sum_{t=0}^{q-2}\left(\frac{B}{B+(k_{\ell,\kappa}+1)\gamma}\right)^t\\&\left.\times L_t\left(-\frac{k_{\ell,\kappa}\gamma(k_{\ell,\kappa}+1)}{B+\gamma(k_{\ell,\kappa}+1)}\right)\right].\end{aligned} \tag{A-7}$$

Based on this solution and after some mathematical manipulations, (10) is obtained and also completes this proof.

Appendix B
Proof for Equation (13)

In this Appendix, the proof for the derivation of (13) is provided. Let us define the following sets $\mathcal{A}=\{p_{1,1},p_{1,2},\ldots,p_{2,1},\ldots,p_{N_t,N_r}\}$ and $\mathcal{B}=\mathcal{A}-p_{\ell,\kappa}$. The probability $P_{\ell\kappa}$ is the probability that the shadowing variable $p_{\ell,\kappa}$ is the maximum of set $\mathcal{A}$. Therefore, in terms of probability theory, this probability can be evaluated as $P_{\ell\kappa}=\Pr\left(p_{\ell,\kappa}=\max\{\mathcal{A}\}\right)=\Pr\left(p_{\ell,\kappa}>\max\{\mathcal{B}\}\right)=\Pr\left(p_{\ell,\kappa}>\gamma_{\mathcal{B}}\right)$. The latter probability can be evaluated as

$$P_{\kappa,\ell}=\int_0^\infty F_{\gamma_{\mathcal{B}}}(y)f_{p_{\kappa,\ell}}(y)dy. \tag{B-1}$$

Substituting (A-5) and (4) in (B-1), and using [15, eq. (3.351/3)] yields (13) and also completes this proof.

Appendix C
Antenna Selection Based on Outdated CSI

In this Appendix, the performance of a communication system with two Tx antennas and a single Rx antenna is studied. For this system, it is assumed that the AS is performed using an estimated version of the received SNR, which is outdated due to the fast varying channel. The scope is to derive an exact expression for the CDF of the output SNR for this scheme. Assuming Rice/IG composite fading and i.i.d. conditions, this CDF can be evaluated as

$$F_{\gamma_{\text{out}}}(\gamma)=\int_0^\infty F_{\gamma_r}(\gamma|y)f_p(y)dy, \tag{C-1}$$

in which $F_{\gamma_r}(\gamma|y)$ denotes the CDF of the actual received output SNR based on the fading variables. Hopefully, for Rice distributed fading variables, this CDF has been previously derived in [23, eq. (19)]. Substituting this equation and (4) in (C-1), integrals of the form given in (A-6) as well as of the following form have appeared

$$\begin{aligned}\mathcal{I}_2=&\int_0^\infty W^{-a}\exp\left(-BW^{-1}\right)\\&\times\gamma\left(\sqrt{2(k+1)},(k+1)W^{-1}\right)dW.\end{aligned} \tag{C-2}$$

This integral can be solved by making a change of variables of the form $W=1/y$ and by using [15, eq. (6.455)]. Based on this solution and after some mathematical procedure, the following expression for the $F_{\gamma_{\text{out}}}(\gamma)$ is finally deduced

$$\begin{aligned}F_{\gamma_{\text{out}}}(\gamma)=&2F_{\gamma_{i,j}}(\gamma_{\text{th}})-\frac{\overline{\gamma}^\alpha}{\Gamma(\alpha)}\sum_{\substack{i,j=0\\ v_1+v_2+v_3=i}}^{\infty}2\mathcal{A}\beta_1^{\beta_3}\\&\times(1-\rho_t^2)^{\alpha+\beta_3}\sum_{n=0}^{\infty}\frac{k^n}{n!}\sum_{p=0}^{n}\frac{e^{-k}}{p!}\left(\frac{1-\rho_t^2}{2-\rho_t^2}\right)^{p+\beta_2}\\&\times\left[(1+(-1)^{v_3})\mathcal{F}(0)-(-1+(-1)^{v_3})\mathcal{F}\left(\frac{1}{2}\right)\right],\end{aligned} \tag{C-3}$$

where

$$\mathcal{A}=\frac{2^{v_3+2h-1}(k+1)^{1+\beta_4}\rho_t^{2h}\left(\frac{k}{(1+\rho_t)^2}\right)^i}{\sqrt{\pi}\,\overline{\gamma}_d^{1+\beta_4}\,(1-\rho_t^2)^{1+2h}\,v_1!\,v_2!\,v_3!\,i!}\exp\left(-\frac{2k}{1+\rho_t}\right),$$

$$\begin{aligned}\mathcal{F}(x)=&\frac{(2\rho_t)^{2x}\Gamma\left(j+x+\frac{1}{2}+\frac{v_3}{2}\right)}{\Gamma\left(2x+2j+1\right)\Gamma\left(x+1+j+\frac{v_3}{2}\right)}\left(\frac{1+k}{1-\rho_t^2}\right)^x\\&\times\frac{\Gamma\left(p+\beta_2+x\right)\Gamma\left(\alpha+\beta_3+x\right)}{(\beta_3+x)\left[\beta_1+\overline{\gamma}(1-\rho_t^2)\right]^{\alpha+\beta_3+x}}\left(\frac{1-\rho_t^2}{2-\rho_t^2}\right)^x\\&\times{}_2F_1\left[1,\alpha+\beta_3+x;\beta_3+x+1;\frac{\beta_1}{\beta_1+\overline{\gamma}(1-\rho_t^2)}\right],\end{aligned}$$

with $\beta_1=(k+1)\gamma_{\text{th}}, \beta_2=v_1+\frac{v_3}{2}+j+1, \beta_3=v_2+\frac{v_3}{2}+j+1$, and ${}_2F_1(\cdot)$ denoting the Gauss hypergeometric function [15, eq. (9.100)].

References

[1] Y. Li, Q. Yin, L. Sun, H. Chen, and H.-M. Wang, "A channel quality metric in opportunistic selection with outdated CSI over Nakagami-m fading channels," *IEEE Trans. Veh. Technol.*, vol. 61, no. 3, pp. 1427–1432, Mar. 2012.

[2] P. S. Bithas, A. G. Kanatas, D. B. da Costa, P. K. Upadhyay, and U. S. Dias, "On the double-generalized gamma statistics and their application to the performance analysis of V2V communications," *IEEE Trans. Commun.*, vol. 66, no. 1, pp. 448–460, Jan. 2018.

[3] A. Yilmaz, F. Yilmaz, M. S. Alouini, and O. Kucur, "On the performance of transmit antenna selection based on shadowing side information," *IEEE Trans. Veh. Technol.*, vol. 62, no. 1, pp. 454–460, Jan. 2013.

[4] S. Hessien, F. S. Al-Qahtani, R. M. Radaydeh, C. Zhong, and H. Alnuweiri, "On the secrecy enhancement with low-complexity large-scale transmit selection in MIMO generalized composite fading," *IEEE Wireless Commun. Lett.*, vol. 4, no. 4, pp. 429–432, Aug. 2015.

[5] E. Erdogan, A. Afana, and S. Ikki, "Multi-antenna down-link cooperative systems over composite multipath/shadowing channels," in *IEEE Wireless Communications and Networking Conference (WCNC)*, Mar. 2017.

[6] Y. Zhou, C. Zhong, S. Jin, Y. Huang, and Z. Zhang, "A low-complexity multiuser adaptive modulation scheme for massive MIMO systems," *IEEE Signal Process. Lett.*, vol. 23, no. 10, pp. 1464–1468, Oct. 2016.

[7] D. Vlastaras *et al.*, "Impact of a truck as an obstacle on vehicle-to-vehicle communications in rural and highway scenarios," in *IEEE 6th International Symposium on Wireless Vehicular Communications (WiVeC)*, Sep. 2014.

[8] Q. Wang, D. W. Matolak, and B. Ai, "Shadowing characterization for 5-GHz vehicle-to-vehicle channels," *IEEE Trans. Veh. Technol.*, vol. 67, no. 3, pp. 1855–1866, Mar. 2018.

[9] S. K. Yoo *et al.*, "The K-μ/inverse gamma fading model," in *IEEE 26th Annual International Symposium on Personal, Indoor, and Mobile Radio Communications (PIMRC)*, 2015, pp. 425–429.

[10] S. K. Yoo and S. L. Cotton, "Composite fading in non-line-of-sight off-body communications channels," in *11th European Conference on Antennas and Propagation (EUCAP)*, Mar. 2017, pp. 286–290.

[11] G. L. Stüber, *Principles of mobile communication*. Springer Science & Business Media, 2011.

[12] L. S. Muppirisetty, T. Svensson, and H. Wymeersch, "Spatial wireless channel prediction under location uncertainty," *IEEE Trans. Wireless Commun.*, vol. 15, no. 2, pp. 1031–1044, Feb. 2016.

[13] T. Abbas, K. Sjöberg, J. Karedal, and F. Tufvesson, "A measurement based shadow fading model for vehicle-to-vehicle network simulations," *International Journal of Antennas and Propagation*, 2015.

[14] M. K. Simon and M.-S. Alouini, *Digital Communication over Fading Channels*, 2nd ed. New York: Wiley, 2005.

[15] I. S. Gradshteyn and I. M. Ryzhik, *Table of Integrals, Series, and Products*, 6th ed. New York: Academic Press, 2000.

[16] A. Goldsmith, *Wireless communications*. Cambridge university press, 2005.

[17] M. Abramowitz and I. A. Stegun, *Handbook of mathematical functions: with formulas, graphs, and mathematical tables*. Courier Corporation, 1964, vol. 55.

[18] R. He, Z. Zhong, B. Ai, and C. Oestges, "Shadow fading correlation in high-speed railway environments," *IEEE Trans. Veh. Technol.*, vol. 64, no. 7, pp. 2762–2772, Jul. 2015.

[19] V. Nikolaidis, N. Moraitis, and A. G. Kanatas, "Dual-polarized narrow-band MIMO LMS channel measurements in urban environments," *IEEE Trans. Antennas Propag.*, vol. 65, no. 2, pp. 763–774, Feb. 2017.

[20] S. Kullback and R. A. Leibler, "On information and sufficiency," *The annals of mathematical statistics*, vol. 22, no. 1, pp. 79–86, 1951.

[21] H. A. David and H. N. Nagaraja, *Order statistics*. Wiley Online Library, 1970.

[22] A. H. Nuttall, "Some integrals involving the Q_M function," *IEEE Trans. Inf. Theory*, vol. 21, no. 1, pp. 95–96, Jan. 1975.

[23] P. S. Bithas, G. P. Efthymoglou, and A. G. Kanatas, "Intervehicular communication systems under co-channel interference and outdated channel estimates," in *IEEE International Conference on Communications (ICC)*, May 2016.